JOURNAL OF SOLID STATE CHEMISTRY **136,** 305–312 (1998)
ARTICLE NO. SC977712

A New Series of Tungstoniobium Monophosphates with an Intersecting Tunnel Structure Closely Related to ReO_3: $ANb_4WO_9(PO_4)_3$ (A = K, Rb, Cs), $KLiNb_5O_9(PO_4)_3$, and $KLi_{1-x}(Nb, W)_5O_9(PO_4)_3$

D. Mezaoui,* M. M. Borel, A. Leclaire, A. Rebbah,* J. Provost, and B. Raveau

Laboratoire CRISMAT – CNRS UMR 6508 – ISMRA, Université de Caen, Boulevard du Maréchal Juin, 14050 Caen Cedex, France; and
**Laboratoire de cristallographie et cristallogénèse, Institut de Chimie, Université des Sciences et de la Technologie Houari Boumedienne, B.P. 32, E1 Alia, Bab Ezzouar Alger, Algeria*

Received July 17, 1997; in revised form November 12, 1997; accepted November 24, 1997

A new series of tungstoniobium monophosphates, $ANb_4WO_9(PO_4)_3$ (A = K, Rb, Cs), $KLiNb_5O_9(PO_4)_3$, and $KLi_{1-x}(Nb, W)_5O_9(PO_4)_3$, has been synthesized. They all crystallize in the space group *Pbam* with $a \approx 15.5$ Å, $b \approx 10.4$ Å, $c \approx 10.5$ Å. Their original intersecting channel structure involving tunnels running along b and c is described by $[M_4P_2O_{19}]_\infty$ layers parallel to (001) interconnected through $[MPO_8]_\infty$ chains. In fact the MO_6 octahedra form a distorted perovskite 3D framework where some octahedra are missing. The study of the transport properties of this phase shows linear behavior for $\ln\sigma$ vs $T^{-1/4}$, characteristic of variable, range-hopping conductivity.

INTRODUCTION

The extraordinary richness of mixed frameworks built from the association of phosphate groups with transition metal octahedra suggests that many compounds with interesting properties remain to be discovered. The tungsten phosphate bronzes discovered twenty years ago (see for a review Refs. 1, 2) are a good example of the utility of such investigations. These materials, which derive from the perovskite by introducing rows or layers of PO_4 or P_2O_7 groups, indeed show remarkable charge density wave properties that are being studied by several groups (3–6). In a similar way, niobium phosphates were investigated more recently (see for a review Ref. 7). The latter differ from the tungsten compounds in that their structure is closely related to those of the hexagonal tungsten bronze (HTB) and tetragonal tungsten bronze (TTB) of Magnéli.

The association of tungsten to niobium in the same matrix is likely to generate original structures with specific properties, in spite of the fact that the only compounds isolated to date, $\alpha\alpha'Nb_{0.787}W_{0.213}OPO_4$ (8) and $K_{3.75}Nb_{8.5-x}W_xO_{14}(PO_4)_4$ (9), are isotypic with pure niobium phosphates. We report here on a new series of monophosphates, $ANb_4WO_9(PO_4)_3$ with A = K, Rb, Cs, that exhibit an original intersecting channel structure. The possibility of intercalating lithium in this framework is also demonstrated, leading to the phosphate $KLi_x(Nb, W)_5O_9(PO_4)_3$, whose electron transport properties are also studied.

EXPERIMENTAL SECTION

Strategy of the Synthesis of Crystal Growth

In order to have a good chance of isolating a new phase in the form of single crystals, numerous compositions in the system K-Nb-W-P-O were systematically tested. In the present study, about 100 compositions with Nb:W and P:W + Nb ratios close to 4/3 and 1/5 and K: P + Nb + W ratios close to 1/20 were investigated. In all cases, a part of tungsten (about 10%) was generally added in the form of metal in order to have some chance of creating a mixed-valence W(V) /W(VI), and also because the reducing conditions are generally favorable to the crystal growth of such compounds.

In these conditions, single crystals of the title phase were obtained from the nominal composition $K_{0.4}Nb_{4.5}W_{3.5}P_{1.8}O_{26.3}$. The growth was performed in two steps. First, an adequate mixture of K_2CO_3, Nb_2O_5, WO_3, $H(NH_4)_2PO_4$ was heated at 673 K in air to eliminate H_2O, CO_2, and NH_3. In a second step, the resulting finely ground powder was mixed with the appropriate amount of tungsten (0.3 mol). This mixture was heated up to 1125 K in an evacuated silica ampoule for 2 days and cooled at 6.25 K per hour to 823 K. The sample was finally quenched to room temperature.

Several sorts of crystals could be extracted from the above products, but they were shown to be either potassium niobates or tungstates or niobotungstates. Only some pale blue crystals could be detached from the walls of the silica tube. Their EDS analysis allowed the presence of silicium to be ruled out and led to the cationic composition

0022-4596/98 $25.00

"$KNb_{4+x}WP_{3-x}$" with $x \cong 0.1$. The latter was confirmed from the structure determination.

At this stage, the structure determination of the single crystal was performed. It revealed that the corresponding formula was $KNb_{4+x}WP_{3-x}O_{21}$, so it was concluded that tungsten and niobium were in their maximum oxidation state.

Single crystals of $RbNb_4WO_9(PO_4)_3$ and $KLi_{0.66}Nb_{4.476}W_{0.524}O_9(PO_4)_3$ were extracted from samples with nominal compositions $RbNb_4WP_3O_{21}$ and $KLiNb_4WP_3O_{21}$ respectively. The synthesis of the latter was also performed in two steps. In the second step, the mixture in an evacuated silica ampoule was heated for the rubidium compound at 1123 K for 15 days and cooled at 44 K h^{-1} to 773 K; the sample was kept at this temperature for a month, then quenched to room temperature. For the "KLi" compound, the sample was heated to 1153 K for 3 days, cooled at 7.5 K h^{-1} to 973 K, and then quenched to room temperature.

Subsequently, we tried to prepare the compounds $ANb_4WP_3O_{21}$ (A = K, Rb, Cs) and $KLiNb_5P_3O_{21}$ in air from an homogeneous and pulverized mixture of K_2CO_3, Li_2CO_3, Nb_2O_5, WO_3, and $H(NH_4)_2PO_4$ in appropriate ratios. The mixture was first heated slowly to 673 K and kept at this temperature for 5 h to eliminate H_2O, CO_2, and NH_3. Then in a second step the mixture was heated to 1153 K and kept at this temperature for 3 days. In these conditions, single phases were synthesized whose powder X-ray diffraction pattern was indexed in an orthorhombic unit cell in agreement with the parameters listed in Table 1.

Energy Dispersive Analysis

The analysis of the elements K, Rb, Nb, W, P, and Si was performed with a Tracor microprobe mounted on a scanning electron microscope.

Atomic Absorption Spectrometry Analysis

This analysis was performed only for potassium and lithium. For the solid phase analysis, the latter was dissolved by boiling in an aqueous mixture of nitric acid and hydrofluoric acid. The solution was analyzed with an atomic absorption spectrometer (Varian Spectra AA 20).

TABLE 1
Cell Parameters of the Isotypic Phases

Compounds	a (Å)	b (Å)	c (Å)	V (Å^3)
$KNb_4WO_9(PO_4)_3$	15.541(2)	10.396(1)	10.391(1)	1679
$RbNb_4WO_9(PO_4)_3$	15.545(2)	10.402(1)	10.397(1)	1681
$CsNb_4WO_9(PO_4)_3$	15.578(2)	10.424(1)	10.419(1)	1692
$KLiNb_5O_9(PO_4)_3$	15.610(2)	10.412(1)	10.482(1)	1703

Electric Measurement

The electric conductivity has been measured between $T = 200$ and 400 K on a sintered bar. Four indium spots have been deposited on the bar using an ultrasonic device. Below $T = 200$ K the resistance of the sample was too large to be measured with the experimental setup (PPMS Quantum design).

X-ray Diffraction Study

Different crystals were tested by film methods using Cu$K\alpha$ radiation. The unit cell parameters of the three compounds were determined by diffractometric techniques at 21°C with a least squares refinement based on 25 reflections with $18° < \theta < 22°$. The data were collected on a CAD4 Enraf Nonius diffractometer with the parameters reported in Table 2. The Laue symmetry *Pmmm* and the systematic extinction $k = 2n + 1$ for 0kl and $h = 2n + 1$ for h01 are

TABLE 2
Summary of Crystal Data, Intensity Measurements, and Structure Refinement Parameters for $KNb_4WO_9(PO_4)_2(P_{0.92}Nb_{0.08}O_4)$ (I), $RbNb_4WO_9(PO_4)_2(P_{0.93}Nb_{0.07}O_4)$ (II), and $KLi_{0.66}Nb_{4.476}W_{0.524}O_9(PO_4)_3$(III)

	I	II	III
	1. Crystal data		
Space group	*Pbam* (no. 55)	*Pbam* (no. 55)	*Pbam* (no. 55)
Cell dimensions			
a (Å)	15.538(1)	15.545(1)	15.584(1)
b (Å)	10.4010(8)	10.4025(7)	10.417(1)
c (Å)	10.4081(9)	10.4073(8)	10.457(1)
Volume (Å)^3	1682.1(2)	1682.9(2)	1697.5(3)
Z	4	4	4
Color	bluish	bluish	black
Size (mm^3)	0.056 × 0.056 × 0.145	0.026 × 0.026 × 0.128	0.064 × 0.064 × 0.083
	2. Intensity measurements		
λ(Mo$K\alpha$)	0.71073 Å	0.71073 Å	0.71073 Å
Scan mode	ω–θ	ω–4/3θ	ω–θ
Scan width (°)	1.1 + 0.35 tan θ	1.05 + 0.35 tan θ	1.2 + 0.35 tan θ
Slit aperture (mm)	1.1 + tan θ	1. + tan θ	1.15 + tan θ
max θ(°)	45	45	45
Standard reflections	3 measured per hour	3 measured per hour	3 measured per hour
Measured reflections	7591	7607	7653
Reflections with $I > 3\sigma$	2391	1777	1293
μ(mm^{-1})	10.1	12.75	8.09
	3. Structure solution and refinement		
Parameters refined	161	155	103
Agreement factors			
R	0.030	0.033	0.036
R_w	0.026	0.030	0.030
Weighting scheme	$w = 1/\sigma^2$	$w = 1/\sigma^2$	$w = 1/\sigma^2$

consistent with the space groups *Pbam* and *Pba*2. The reflections were corrected for Lorentz and polarization effects and for absorption and secondary extinction. The structure of $KNb_4WO_9(PO_4)_3$ was solved with the heavy atom method and the Harker peaks show that the space group is *Pbam*. First only Nb atoms were introduced in the octahedra and P atoms in the tetrahedra. However after refinement of atomic coordinates, the refinement of the occupancy factors showed an excess of electrons on the octahedral sites and on the P(1) tetrahedral site. So tungsten and niobium were put in the octahedra and niobium and phosphorus on the P(1) site. The refinement of the atomic parameters, the anisotropic thermal factors, and the ratio of the mixed atoms led to $R = 0.030$, $R_w = 0.026$, and the data listed in Table 3a. The structure of the two other compounds was solved by isotypie with the first one. The Li atoms were located on a difference Fourier synthesis. The refinement of both structures led to $R = 0.033$ and $R_w = 0.030$ for the Rb phase and $R = 0.036$ and $R_w = 0.030$ for the "LiK" phase. The corresponding atomic coordinates are listed in Tables 3b and 3c.

TABLE 3a
$KNb_4WO_9(PO_4)_2(P_{0.92}Nb_{0.08}O_4)$: Atomic Parameters

Atom	x	y	z	B_{eq} (Å^2)	Site	Occup.
M(1)	0.07659(2)	0.14012(4)	0.18164(3)	0.847(8)	8i	[a]
M(2)	0.22272(2)	0.42815(5)	0.17648(5)	0.75(1)	8i	[b]
M(3)	0.29166(4)	0.33124(6)	0.5000	0.66(2)	4h	[c]
P(1)	0.1214(1)	0.1270(2)	0.5000	0.51(4)	4h	[d]
P(2)	0.37977(8)	0.2132(1)	0.2291(1)	0.65(3)	8i	1.00
K(1)	0.0000	0.5000	0.0000	3.4(1)	2c	1.00
K(2)	0.0082(6)	0.4030(9)	0.5000	4.1(3)	4h	0.33(1)
K(3)	0.068(2)	0.481(3)	0.5000	8.8(2)	4h	0.17(1)
O(1)	0.0749(2)	0.1791(4)	0.3809(3)	0.9(1)	8i	1.00
O(2)	0.0000	0.0000	0.2094(5)	1.0(2)	4e	1.00
O(3)	0.0704(3)	0.1251(5)	0.0000	1.0(1)	4g	1.00
O(4)	0.1351(2)	0.3113(3)	0.1590(3)	0.9(1)	8i	1.00
O(5)	0.1765(2)	0.0567(4)	0.2052(3)	1.0(1)	8i	1.00
O(6)	−0.0305(2)	0.2623(4)	0.1782(4)	1.0(1)	8i	1.00
O(7)	0.2308(2)	0.4010(4)	0.3663(3)	0.9(1)	8i	1.00
O(8)	0.3133(2)	0.2950(4)	0.1568(3)	0.9(1)	8i	1.00
O(9)	0.1386(2)	0.5699(3)	0.2044(4)	1.0(1)	8i	1.00
O(10)	0.2310(3)	0.4698(5)	0.0000	1.1(2)	4g	1.00
O(11)	0.3768(3)	0.4789(5)	0.5000	1.1(2)	4h	1.00
O(12)	0.2167(3)	0.1744(5)	0.5000	0.9(1)	4h	1.00
O(13)	0.3740(2)	0.2379(4)	0.3733(3)	0.9(1)	8i	1.00

[a] M(1) = 0.635(4)Nb + 0.365(4)W
[b] M(2) = 0.885(4) Nb + 0.115(4) W
[c] M(3) = 0.960(4) Nb + 0.040(4) W
[d] P(1) = 0.924(4) P + 0.076(4) Nb

Note: Anisotropically refined atoms are given in the form of the isotropic equivalent displacement parameter, defined as:

$$B = \frac{4}{3}\sum_i\sum_j \mathbf{a}_i \cdot \mathbf{a}_j \cdot \beta_{ij}$$

TABLE 3b
$RbNb_4WO_9(PO_4)_2(P_{0.93}Nb_{0.07}O_4)$: Atomic Parameters

Atom	x	y	z	B_{eq} (Å^2)	Site	Occup.
M(1)	0.07637(3)	0.14106(5)	0.18216(5)	0.884(2)	8i	[a]
M(2)	0.22285(4)	0.42834(6)	0.17685(7)	0.829(1)	8i	[b]
M(3)	0.29316(6)	0.33324(9)	0.5	0.426(2)	4h	[c]
P(1)	0.1220(1)	0.1294(2)	0.5	0.450(6)	4h	[d]
P(2)	0.3792(1)	0.2138(2)	0.2297(2)	0.505(5)	8i	1.00
Rb(1)	0.0	0.5	0.0	1.7(5)	2c	1.00
Rb(2)	0.022(1)	0.445(1)	0.5000	6.9(4)[e]	4h	0.33(2)
Rb(3)	0.056(1)	0.478(2)	0.5000	3.5(5)[e]	4h	0.17(2)
O(1)	0.0759(3)	0.1804(5)	0.3803(5)	0.7(1)	8i	1.00
O(2)	0.0	0.0	0.2116(7)	0.9(2)	4e	1.00
O(3)	0.0698(4)	0.1263(7)	0.0000	0.5(2)	4g	1.00
O(4)	0.1352(3)	0.3113(5)	0.1591(5)	0.9(2)	8i	1.00
O(5)	0.1762(2)	0.0576(5)	0.2026(5)	0.8(2)	8i	1.00
O(6)	−0.0311(3)	0.2608(5)	0.1786(5)	0.8(1)	8i	1.00
O(7)	0.2313(3)	0.4030(5)	0.3659(5)	0.7(1)	8i	1.00
O(8)	0.3133(3)	0.2954(5)	0.1570(5)	0.7(1)	8i	1.00
O(9)	0.1393(3)	0.5688(5)	0.2051(5)	0.8(1)	8i	1.00
O(10)	0.2306(5)	0.4712(7)	0.0	1.1(2)	4g	1.00
O(11)	0.3752(5)	0.4829(7)	0.5	0.8(2)	4h	1.00
O(12)	0.2160(5)	0.1767(7)	0.5	0.9(2)	4h	1.00
O(13)	0.3730(3)	0.2392(4)	0.3729(4)	0.8(1)	8i	1.00

[a] M(1) = 0.633(6)Nb + 0.367(6) W
[b] M(2) = 0.885(6)Nb + 0.115(6) W
[c] M(3) = 0.965(6)Nb + 0.035(6) W
[d] P(1) = 0.935(6)P + 0.065(6) Nb
[e] Isotropically refined atoms

Note: Anisotropically refined atoms are given in the form of the isotropic equivalent displacement parameter, defined as:

$$B = \frac{4}{3}\sum_i\sum_j \mathbf{a}_i \cdot \mathbf{a}_j \cdot \beta_{ij}$$

RESULTS AND DISCUSSION

Description of the $[M_5P_3O_{21}]_\infty$ Framework

The projections of the framework along **c** (Fig. 1) and **b** (Fig. 2) show that these new phases consist of corner-sharing MO_6 octahedra and PO_4 tetrahedra, each tetrahedron being connected to four MO_6 octahedra. This original structure can be described as a monophosphate with the ideal formula $AM_5O_9(PO_4)_3$. The so-formed $[M_5P_3O_{21}]_\infty$ framework delimits six-sided tunnels built of rings of four octahedra and two tetrahedra running along **c** (Fig. 1) and **b** (Fig. 2). The geometry of the first ones is similar to that observed in brownmillerite (10), whereas the second ones are similar to the tunnels observed in the HTBs.

In fact this framework is built of double $[M_4P_2O_{19}]_\infty$ layers parallel to (001) interconnected through $[MPO_8]_\infty$ chains (Fig. 2). Each $[M_4P_2O_{19}]_\infty$ double layer consists of two single $[M_4P_2O_{21}]_\infty$ layers that are enanthiomorphic. The geometry of such a $[M_4P_2O_{21}]_\infty$ layer is shown in Fig. 3 as a projection along b. The latter is built entirely of six-sided rings "$M_4P_2O_{26}$" derived from the HTBs by

TABLE 3c
$KLi_{0.66}Nb_{4.476}W_{0.524}O_9(PO_4)_3$: Atomic Parameters

Atom	x	y	z	B_{eq} (Å^2)	Site	Occup.
M(1)	0.07721(5)	0.13932(8)	0.18082(7)	0.70(2)[c]	8i	[a]
M(2)	0.22227(5)	0.42904(8)	0.17580(9)	0.65(2)[c]	8i	[b]
Nb(3)	0.28545(9)	0.3289(6)	0.5000	0.66(2)[c]	4h	1.00
P(1)	0.1216(2)	0.1202(2)	0.5000	0.42(9)[c]	4h	1.00
P(2)	0.3799(2)	0.2142(2)	0.2309(1)	0.62(7)[c]	8i	1.00
K(1)	0.0000	0.5000	0.0000	3.9(3)[c]	2c	1.00
K(2)	0.009(1)	0.394(2)	0.5000	4.8(6)	4h	0.34(1)
K(3)	0.094(2)	0.496(3)	0.5000	4.0(1)	4h	0.16(1)
Li	−0.034(3)	0.192(5)	0.5000	2.4(1)	4h	0.66(1)
O(1)	0.0729(4)	0.1722(7)	0.3830(6)	1.0(1)	8i	1.00
O(2)	0.0000	0.0000	0.208(1)	1.2(2)	4e	1.00
O(3)	0.0717(6)	0.1241(9)	0.0000	0.9(2)	4g	1.00
O(4)	0.1355(4)	0.3105(6)	0.1606(6)	0.7(1)	8i	1.00
O(5)	0.1780(4)	0.0570(7)	0.2069(6)	0.9(2)	8i	1.00
O(6)	−0.0304(4)	0.2618(6)	0.1805(7)	0.8(1)	8i	1.00
O(7)	0.2285(4)	0.4009(6)	0.3664(6)	1.1(2)	8i	1.00
O(8)	0.3139(4)	0.2964(7)	0.1596(7)	1.1(2)	8i	1.00
O(9)	0.1393(4)	0.5721(7)	0.2051(6)	1.0(1)	8i	1.00
O(10)	0.2306(6)	0.4711(9)	0.0000	1.1(2)	4g	1.00
O(11)	0.3765(7)	0.472(1)	0.5000	1.1(2)	4h	1.00
O(12)	0.2149(6)	0.1685(5)	0.5000	0.8(1)	4h	1.00
O(13)	0.3752(4)	0.2398(7)	0.3754(6)	0.8(1)	8i	1.00

[a] M(1) = 0.780(5)Nb + 0.220(5)W
[b] M(2) = 0.958(4)Nb + 0.042(4)W
[c] Anisotropically refined atoms

Note: Anisotropically refined atoms are given in the form of the isotropic equivalent displacement parameter, defined as:

$$B = \frac{4}{3}\sum_i \sum_j \mathbf{a}_i \cdot \mathbf{a}_j \cdot \beta_{ij}$$

replacing two MO_6 octahedra out of six with PO_4 tetrahedra. These rings, which involve the M(1) and M(2) octahedra and the P(2) tetrahedra, share the equatorial apices of their polyhedra so that each P(2) tetrahedron is linked to three M octahedra (2 M(1) + 1 M(2)), each M(1) octahedron is linked to two M(2) octahedra and two P(2) tetrahedra, and each M(2) octahedron is linked to three M octahedra (2 M(2) + 1 M(1)) and one P(2) tetrahedron. The third apices of the P(2) tetrahedra of two successive enanthiomorphic layers are oriented in opposite directions along c; thus, two adjacent $[M_4P_2O_{21}]_\infty$ layers share solely the apical corners of their octahedra to form the $[M_4P_2O_{19}]_\infty$ double layer (Fig. 2).

In the $[MPO_8]_\infty$ chains that ensure the connection between two $[M_4P_2O_{19}]_\infty$ layers, one P(1) tetrahedron alternates with one M(3) octahedron. As shown from the projection along **c** (Fig. 4), these chains running along **b** are strongly undulated and isolated one from each other. Each P(1) tetrahedron shares its two apical apices with two M(2) octahedra from two different $[M_4P_2O_{19}]_\infty$ layers (Fig. 2). In the same way, each M(3) octahedron shares four apices with

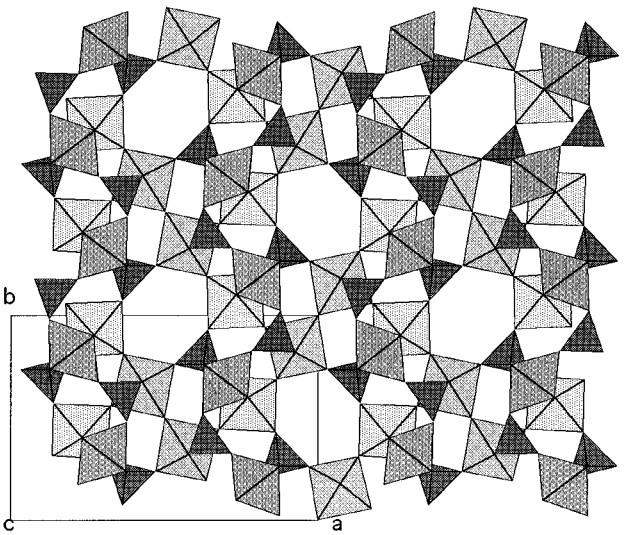

FIG. 1. Projection of the structure of $KNb_4WO_9(PO_4)_3$ along **a**, showing the connection of the polyhedra delimiting the channels. The K/Rb atoms are omitted.

two M(1) octahedra and two P(2) tetrahedra from two different $[M_4P_2O_{19}]_\infty$ layers. Note that a similar mode of connection of double layers through $[NbPO_8]_\infty$ chains was previously observed in the monophosphate $Na_4Nb_8O_9(PO_4)_6$ (11).

One interesting feature concerns the distribution of the metallic species over the different sites (Table 2). The W and Nb cations are not distributed at random in spite in their similarity. Tungsten sits preferentially on the M(1) sites (36% for "K" and "Rb" and 22% for "LiK"), whereas the M(2) sites contain 12% W for "K" and "Rb" phases and 4% for "KLi". The M(3) site that characterizes the $[MPO_8]_\infty$ chains is tungsten-free in the "KLi" phase and contains only 4% W in the other two phases. Note also that the P(1) site is partially occupied by niobium (8%) in the K and Rb compound. Nevertheless these variations of the tetrahedral and octahedral site occupancy induce very small changes in the M–O and P–O distances (Table 4).

Distribution and Coordination of the Intercalated Cations

Four sites are available for the alkaline ions; three can contain K or Rb, the fourth contains only Li. The Al site located in the $[M_4P_2O_{19}]_\infty$ double layers (Fig. 3) exhibits a twelve-fold coordination (4 + 4 + 4) derived from the one observed on the perovskite structure, with rather large A1–O distances ranging from 3.11 and 3.32 Å. In the three structures, this site is fully occupied by potassium or rubidium with thermal factors ranging from 3.5 to 1.7 Å^2 respectively, in agreement with the size of these cations. The second potassium or rubidium atom is distributed over two sites, A2 and A3, but prefers the A2 site. These two sites are

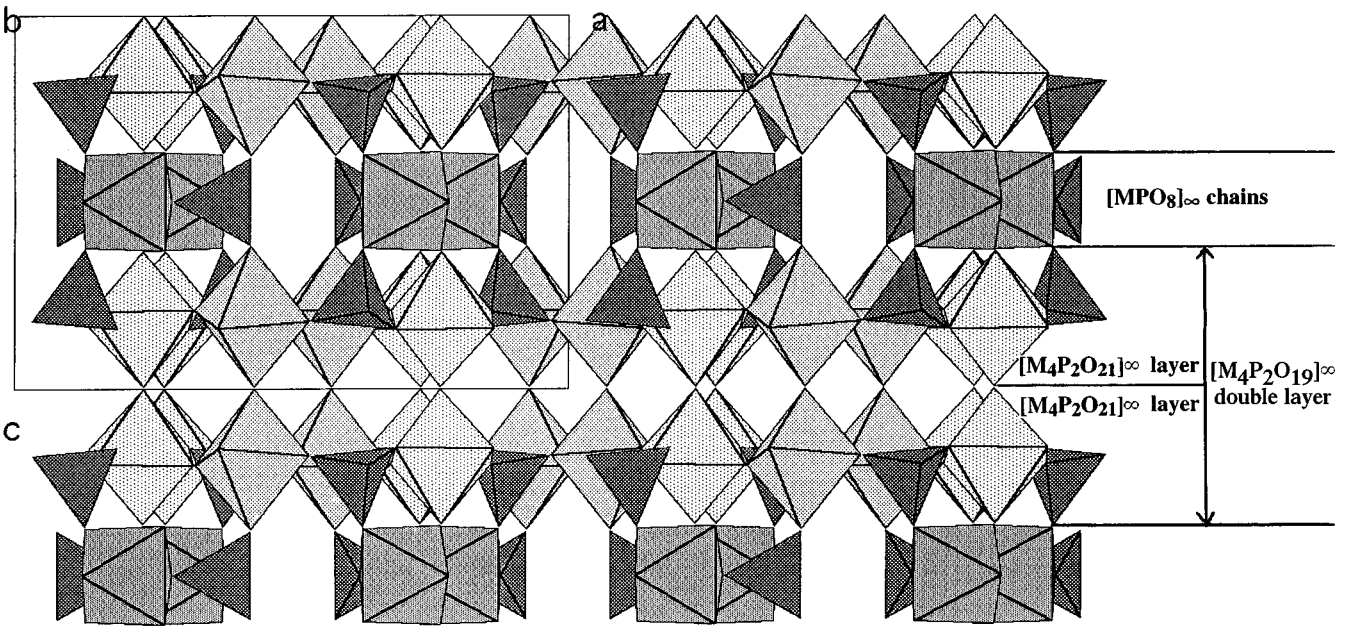

FIG. 2. Projection of the structure of $KNb_4WO_9(PO_4)_3$ along **b**, showing the stacking of high density layers alternating with low density layers. The K/Rb atoms are omitted.

located in very large cages, so they are off-center near the walls of the tunnels (Fig. 6). In the A2 sites the K^+ or Rb^+ cations exhibit a four-fold coordination, the four oxygen atoms being located on the same side with respect to the cation. In contrast, two different coordinations are observed for the cation of the A3 site: K^+ exhibits a four-fold coordination in the "K" compound, whereas K^+ and Rb^+ exhibit a six-fold coordination in the "KLi" and Rb compounds. One also observes that the A–O distances are significantly shorter for A2 and A3 sites than for the A1 site, with distances ranging from 2.80 to 3.28 Å for A2, and from 2.71 to 3.35 Å for A3.

The lithium cation is located in the bottleneck of the tunnels running along **b** (Fig. 6), where it adopts an abnormal distorted square pyramidal coordination, with four equatorial oxygen atoms at 2.05–2.07 Å and the apical

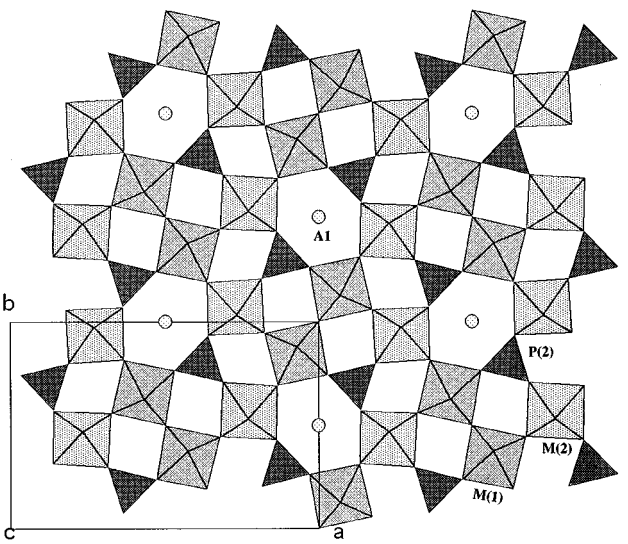

FIG. 3. Projection of $[M_4P_2O_{21}]_\infty$ layer along **c** containing the A1 sites.

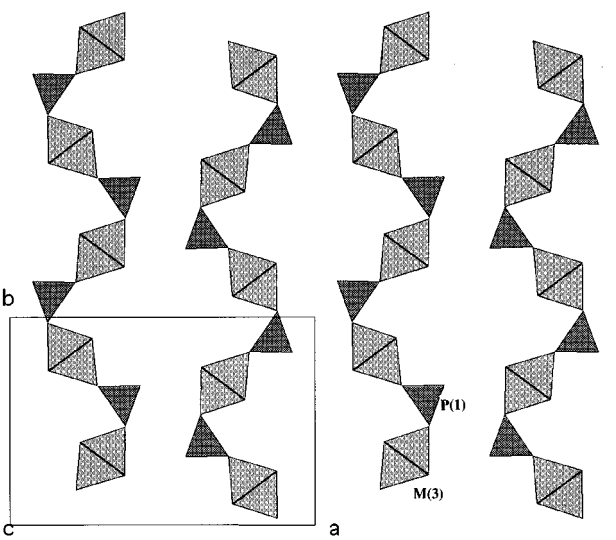

FIG. 4. The projection of $[MPO_8]_\infty$ chains along **c** showing the sequence of large cages followed by bottlenecks.

TABLE 4
Distances (Å) in the Polyhedra

	I(K)	II(Rb)	III($KLi_{0.66}$)
	OCTAHEDRON M(1) O_6		
M(1)–O(1)	2.113(4)	2.102(5)	2.143(7)
M(1)–O(2)	1.904(1)	1.912(1)	1.906(2)
M(1)–O(3)	1.899(1)	1.905(1)	1.900(2)
M(1)–O(4)	2.013(4)	2.007(4)	2.012(6)
M(1)–O(5)	1.795(4)	1.791(5)	1.810(7)
M(1)–O(6)	2.094(4)	2.084(5)	2.11(1)
	OCTAHEDRON M(2) O_6		
M(2)–O(4)	1.834(4)	1.836(5)	1.839(6)
M(2)–O(5^{i})	2.081(4)	2.083(5)	2.073(7)
M(2)–O(7)	2.000(4)	1.989(5)	2.016(7)
M(2)–O(8)	1.985(4)	1.983(5)	1.994(7)
M(2)–O(9)	1.992(4)	1.977(5)	1.996(7)
M(2)–O(10)	1.892(4)	1.897(2)	1.894(3)
	OCTAHEDRON M(3) O_6		
M(3)–O(7)	1.832(4)	1.844(5)	1.817(7)
M(3)–O(7^{ii})	1.832(4)	1.844(5)	1.817(7)
M(3)–O(11)	2.027(5)	2.013(7)	2.06(1)
M(3)–O(12)	2.004(5)	2.022(7)	2.00(1)
M(3)–O(13)	2.078(4)	2.062(5)	2.125(7)
M(3)–O(13^{ii})	2.078(4)	2.062(5)	2.125(7)
	TETRAHEDRON P(1) O_4		
P(1)–O(1)	1.535(4)	1.532(5)	1.538(7)
P(1)–O(1^{i})	1.535(4)	1.532(5)	1.538(7)
P(1)–O(11^{iii})	1.540(6)	1.524(7)	1.55(1)
P(1)–O(12)	1.561(5)	1.543(7)	1.54(1)
	TETRAHEDRON P(2) O_4		
P(2)–O(6^{iv})	1.514(4)	1.515(5)	1.515(7)
P(2)–O(8)	1.535(4)	1.531(5)	1.532(7)
P(2)–O(9^{iii})	1.540(4)	1.556(5)	1.534(8)
P(2)–O(13)	1.525(4)	1.516(5)	1.537(7)
	SITE A1		
K/Rb(1)–O(4)	3.316(4)	3.318(5)	3.316(4)
O(4^{vi})	3.316(4)	3.318(5)	3.316(4)
O(4^{v})	3.316(4)	3.318(5)	3.316(4)
O(4^{vii})	3.316(4)	3.318(5)	3.316(4)
O(6)	3.127(4)	3.143(5)	3.127(4)
O(6^{v})	3.127(4)	3.143(5)	3.127(4)
O(6^{vi})	3.127(4)	3.143(5)	3.127(4)
O(6^{vii})	3.127(4)	3.143(5)	3.127(4)
O(9)	3.113(4)	3.124(5)	3.113(4)
O(9^{v})	3.113(4)	3.124(5)	3.113(4)
O(9^{vi})	3.113(4)	3.124(5)	3.113(4)
O(9^{vii})	3.113(4)	3.124(5)	3.113(4)

TABLE 4—*Continued*

	I(K)	II(Rb)	III($KLi_{0.66}$)
	SITE A2		
K/Rb(2)–O(1)	2.835(9)	3.14(1)	2.80(2)
O(13^{viii})	2.870(9)	3.14(1)	2.83(2)
O(1^{ii})	2.835(9)	3.28(2)	2.80(2)
O(13^{ix})	2.870(9)	3.28(2)	2.83(2)
	SITE A3		
K/Rb(3)–O(7)	3.01(2)	3.35(2)	2.71(3)
O(7^{ii})	3.01(2)	3.35(2)	2.71(3)
O(13^{i})	3.11(3)	3.15(2)	2.90(3)
O(13^{x})	3.11(3)	3.15(2)	2.90(3)
O(9)	3.40(3)	3.21(2)	3.26(2)
O(9^{ii})	3.40(3)	3.21(2)	3.26(2)
	SITE A4		
Li–O(1)			2.07(4)
Li–O(1^{ii})			2.07(4)
Li–O(13^{viii})			2.05(4)
Li–O(13^{ix})			2.05(4)
Li–O(11^{ix})			2.21(6)
	Symmetry codes		
i:	$\frac{1}{2} - x$	$\frac{1}{2} + y$	z
ii:	x	y	$1 - z$
iii:	$\frac{1}{2} - x$	$-\frac{1}{2} + y$	z
iv:	$\frac{1}{2} + x$	$\frac{1}{2} - y$	z
v:	$-x$	$1 - y$	$-z$
vi:	$-x$	$1 - y$	z
vii:	x	y	$-z$
viii:	$-\frac{1}{2} + x$	$\frac{1}{2} - y$	$1 - z$
ix:	$-\frac{1}{2} + x$	$\frac{1}{2} - y$	z
x:	$\frac{1}{2} - x$	$\frac{1}{2} + y$	$1 - z$

oxygen at 2.21 Å. Such a rather rare coordination has already been observed in $Li_2Na(MoO)_2(PO_4)_3$ (12), γLiO_3 (13), and $LiBO_2$ (14).

The interatomic distances between the various A sites, including the equivalent ones, means that they cannot all be occupied simultanously. This is the case for A2 and A3 sites, which can only be 50% occupied, because two equivalent A2 (or A3) sites in the same cage would be too close to each other, leading to A–A distances of 2.22 and 2.92 Å for A2 and A3 respectively. Similarly, in the "KLi" compound, A3 and Li sites can be occupied simultaneously, but cannot be occupied when a cation sits in the A2 site due to the short A2–Li (2.21 Å) and A2–A3 (1.69 Å) distances. Thus when the A2 site is empty, the A3 site can be 50% occupied and the lithium site fully occupied. This possibility is confirmed by the synthesis of the monophosphate $KLiNb_5O_9(PO_4)_3$. Finally it is remarkable that the positions of the atoms located

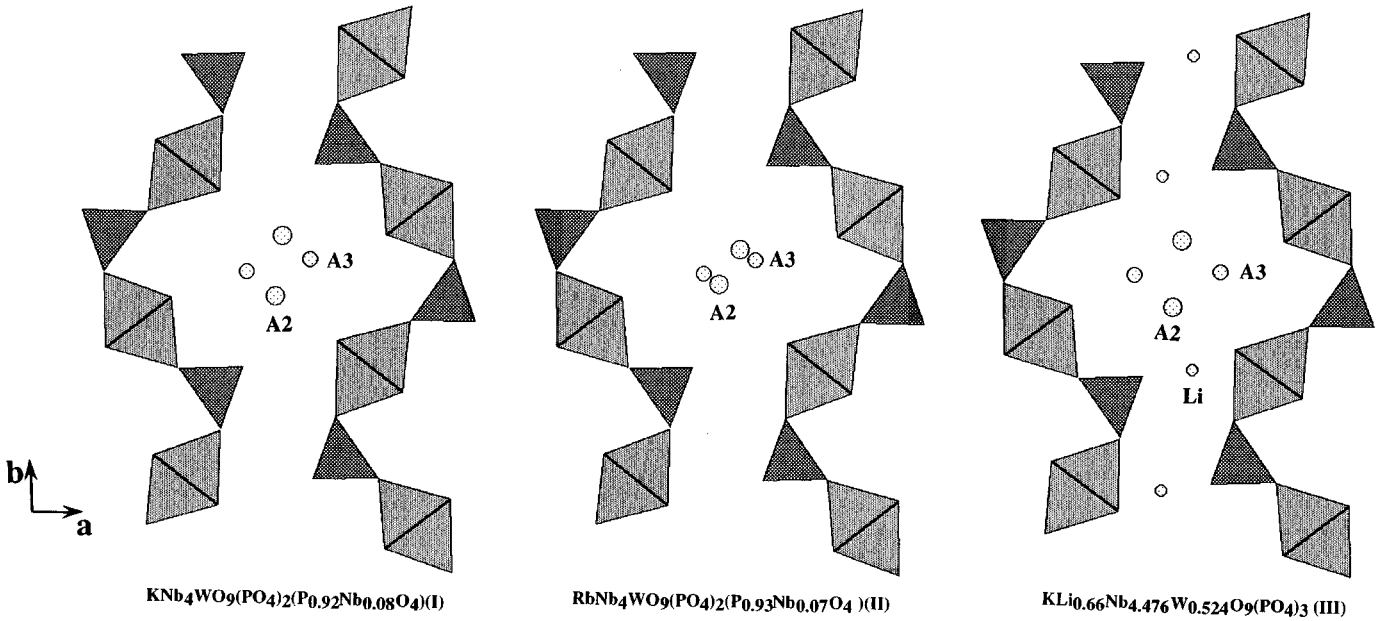

FIG. 5. Localization of the cationic sites in the $[MPO_8]_\infty$ layer through the three compounds.

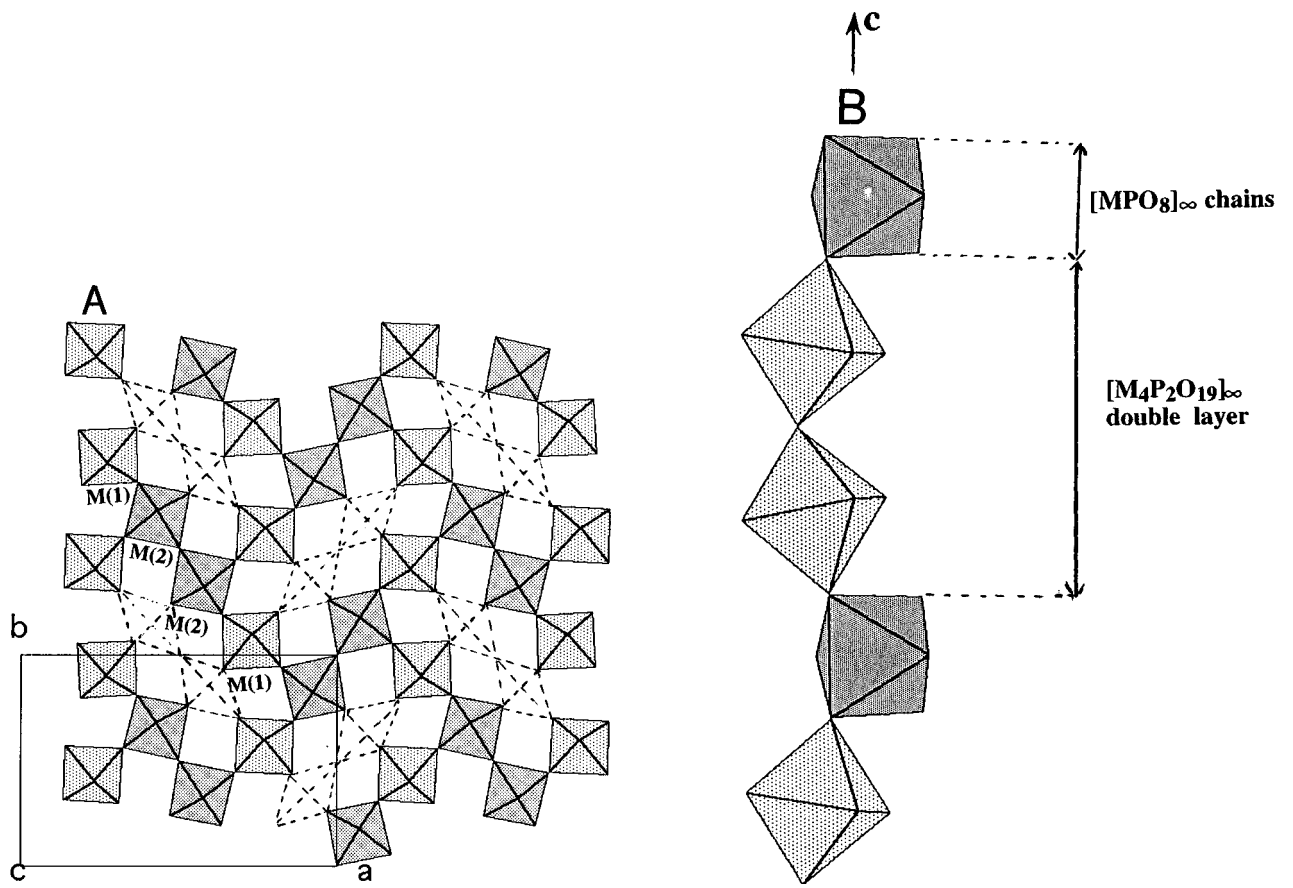

FIG. 6. (a) Projection of $[M_4P_2O_{21}]_\infty$ layer along **c** (omitting the PO_4 tetrahedra), illustrating the close relationship with the ReO_3 structure; (b) $[MO_5]_\infty$ chain running along **c** perpendicular to the $[M_4P_2O_{21}]_\infty$ layer.

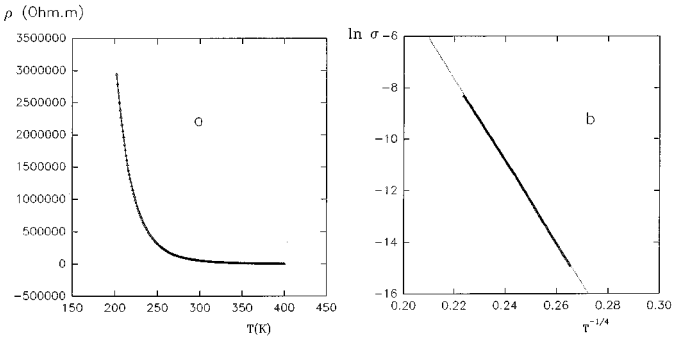

FIG. 7. Experimental conductivity data. Theoretical behavior according to the VRH model (straight line). (a) Plot of resistivity vs T; (b) Plot of the logarithm of the conductivity vs $T^{-1/4}$.

in the A3 site are strongly influenced by the presence of lithium. The Li^+ cations push the K^+ ions of this site closer to the walls of the cage as seen by the significant variation of the atomic coordinates of potassium, the decrease in the thermal factor of K^+ (4 Å^2) compared to the $KNb_4WO_9(PO_4)_3$ phosphate (8.8 Å^2), and the decrease of the K–O distances (Table 4).

Relationships with the ReO_3-Type Structure

A more detailed analysis of the structure shows that the $[M_4P_2O_{19}]_\infty$ double layers are closely related to the ReO_3-type structure. One of the two enanthiomorphic $[M_4P_2O_{21}]_\infty$ single layers forming such double layers is presented in Fig. 5a, where the PO_4 tetrahedra have been omitted. It clearly appears that the $[M_4O_{19}]_\infty$ framework of such a layer can be described as a distorted ReO_3-type framework in which two octahedra out of six are missing (dashed lines on Fig. 5a). Thus the structure of this new phase consists of double distorted ReO_3-type layers, where two MO_6 octahedra out of six are missing. Along **c**, two $[M_4O_{19}]_\infty$ double layers are interconnected through MO_6 octahedra belonging to the $[MPO_8]_\infty$ chains as schematized in Fig. 5b. Thus, these structures are remarkable in that they exhibit a pure octahedral three-dimensional framework allowing physical properties.

Electric Measurements

The three compounds have the same structure, a tridimensional network of distorted ReO_3-type layers with missing octahedra. The $KLiNb_4WO_9(PO_4)_3$ compound contains only mixed-valent Nb/W. This situation is favorable to electronic delocalization, and the electronic conductivity of this compound has been measured between 200 and 400 K. The resistivity vs temperature curve is shown in Fig. 7a. The resistivity was too large for $T < 200$ K to be measured with our setup. The logarithm of the conductivity does not obey classic, thermally activated behavior for a semiconductor. Ln σ vs $T^{-1/4}$ shows linear behavior (Fig. 7b) with variable, range-hopping conductivity. This behavior is compatible with the disordered distribution of W and Nb cations in the structure.

REFERENCES

1. B. Raveau, *Proc. Indian Acad. Sci.* (*Chem. Sci.*) **96,** 419 (1989).
2. M.-M. Borel, M. Goreaud, A. Grandin, Ph. Labbe, A. Leclaire, and B. Raveau, *Eur. J. Solid State Inorg. Chem.* **28,** 93 (1991).
3. E. Wang, M. Greenblatt, I. E. I. Rachidi, E. Canadell, and M. H. Wangho, *J. Solid State Chem.* **81,** 173 (1989).
4. Z. S. Teweldemedhin, K. V. Ramanujachary, and M. Greenblatt, *Phys. Rev. B* **46,** 7897 (1992).
5. P. Foury, J. P. Pouget, Z. S. Teweldemedhin, E. Wang, M. Greenblatt, and D. Groult, *J. Physique IV*, **3,** 133 (1993).
6. C. Le Touzé, G. Bonfait, C. Schlenker, J. Dumas, M. Almeida, M. Greenblatt, and Z. S. Teweldemedhin, *J. Physique I*, **5,** 437 (1995).
7. B. Raveau, M.-M. Borel, A. Leclaire, and A. Grandin, *Int. J. Modern Phys. B* **7,** 4109 (1993).
8. D. Mezaoui, A. Leclaire, M.-M. Borel, and B. Raveau, *Z. Kristallogr.* **212,** 837 (1997).
9. A. Leclaire, M.-M. Borel, D. Mezaoui, H. Rebbah, and B. Raveau, *C.R. Acad. Sci. Paris, Série II*, **323,** 679 (1996).
10. E. F. Bertaut, P. Blum, and A. Sagnières, *Acta Crystallogr.* **12,** 149 (1959).
11. A. Benabbas, M.-M. Borel, A. Grandin, A. Leclaire, and B. Raveau, *J. Solid State Chem.* **89,** 75 (1990).
12. S. Ledain, A. Leclaire, M. M. Borel, and B. Raveau, *J. Solid State Chem.* **129,** 298 (1997).
13. J. M. Crettez, E. Coquet, J. Pannetier, J. Bouillot, and M. Durand-Le Floch, *J. Solid State Chem.* **56,** 133 (1995).
14. A. Kirbel, G. Willand, and R. F. Stewart, *Acta Crystallogr. Sect. B* **39,** 175 (1983).